Structure of ${}^{10}_{\Lambda}$Be and ${}^{10}_{\Lambda}$B hypernuclei studied with the four-body cluster model

Emiko Hiyama, and Yasuo Yamamoto

Nishina Center for Accelerator-Based Science, Institute for Physical and Chemical Research (RIKEN), Wako, Saitama, 351-0198,Japan

The structure of the isodoublet hypernuclei, ${}^{10}_{\Lambda}$B and ${}^{10}_{\Lambda}$Be within the framework of an $\alpha+\alpha+\Lambda+N$ four-body cluster model is studied. Interactions between the constituent subunits are determined so as to reproduce reasonably well the observed low-energy properties of the $\alpha\alpha$, αN, $\alpha\Lambda$, $\alpha\alpha\Lambda$ and $\alpha\alpha N$ subsystems. Furthermore, the two-body ΛN interaction is adjusted so as to reproduce the 0^+-1^+ splitting of ${}^{4}_{\Lambda}$H. The Λ binding energies of ${}^{10}_{\Lambda}$B and ${}^{10}_{\Lambda}$Be are 8.76 MeV and 8.94 MeV, respectively. The energy splitting of the 1^--2^- levels in ${}^{10}_{\Lambda}$B is 0.08 MeV, which does not contradict the experimental report in BNL-E930. An even-state ΛN charge symmetry breaking (CSB) interaction determined from the A=4 systems works repulsively by +0.1 MeV (attractively by −0.1 MeV) in ${}^{10}_{\Lambda}$Be (${}^{10}_{\Lambda}$B). We discuss a possibility that an odd-state CSB interaction improves the fitting to the experimental data of $A = 10$ double Λ hypernuclei.

§1. Introduction

One of the primary goals in hypernuclear physics is to extract information about baryon-baryon interactions in a unified way. By making use of the hyperon(Y)-nucleon(N) scattering data and the rich complementary NN data, several types of YN/YY interaction models have been proposed that are based on the SU(3) and SU(6) symmetries. However, these YN/YY interaction models have a great deal of ambiguity at present, since the YN scattering experiments are extremely limited and there is no YY scattering data. Therefore, it is important to extract useful information on YN/YY interactions from studies of hypernuclear structure. In the case of the ΛN sector, the results of high-resolution γ-ray experiments have been quite important for such a purpose, where level structures of Λ hypernuclei are determined within keV systematically.

Theoretically, a powerful calculation method, the Gaussian Expansion Method (GEM),[1)] was proposed as a means to perform accurate calculations of the structure for three- and four-body system. GEM has been used to successfully study structures for a variety of few-body systems in atomic, baryonic and quark-level problems. In order to extract information about the ΛN interaction, this method was applied to s- and p-shell Λ-hypernuclei represented by three- and/or four-body models composed of Λ and nuclear-cluster subunits, and the spin-dependent parts of the ΛN interactions were determined using the results of the γ-ray experiments: In Ref.2), the ΛN spin-orbit interactions were determined from the observed energies of spin-doublet states in ${}^{9}_{\Lambda}$Be (${}^{13}_{\Lambda}$C) represented by the $\alpha\alpha\Lambda$ ($\alpha\alpha\alpha\Lambda$) cluster model. In Ref.3), the ΛN spin-spin interactions in even- and odd-states were investigated through the combined analyses for ${}^{4}_{\Lambda}$H (${}^{4}_{\Lambda}$He) and ${}^{7}_{\Lambda}$Li ($\alpha pn\Lambda$), where the above spin-orbit interaction was used as an input. These works indicate that we are now entering a new

stage to extract detailed information on the ΛN interaction by combining few-body calculations and γ-ray experimental data.

In this work, on the basis of our previous studies, we investigate structures of ${}^{10}_{\Lambda}$Be ($\alpha\alpha n\Lambda$) and ${}^{10}_{\Lambda}$B ($\alpha\alpha p\Lambda$) and properties of the underlying ΛN interaction. These Λ hypernuclei have provided us many interesting insights so far. For example, aiming to study ΛN spin-dependent interactions, the high-resolution γ-ray experiment was performed to measure the splitting of the 1^--2^- levels of ${}^{10}_{\Lambda}$B in BNL-E930.[4] However, they observed no γ transition between the ground state doublet: this suggests that the 1^--2^- energy splitting in ${}^{10}_{\Lambda}$B is less than 100 keV, or the ground state of this hypernucleus is a 2^- state.

In order to explain the energy splitting in this hypernucleus, the shell model calculation including $\Lambda N - \Sigma N$ coupling explicitly was performed by Millener,[5] where observed spectra of p-shell hypernuclei were reproduced systematically with the five parameters giving $p_N s_\Lambda$ two-body matrix elements. When this analysis was applied straightforwardly to ${}^{10}_{\Lambda}$B, they obtained the ground 1^- state and the 1^--2^- splitting energy of 120 keV.[6] This splitting is slightly larger than the above limitation energy 100 keV to observe the M1 transition from 2^- to 1^- state. They showed also that another interaction set could give rise to the far smaller value 34 keV[6] and they mentioned the $\Lambda\Sigma$ coupling interaction in this case was unrealistic. Thus, it is not so simple to reproduce the splitting energy less than 100 keV in the shell model analysis. It is very important to investigate the level structures of ${}^{10}_{\Lambda}$Be and ${}^{10}_{\Lambda}$B within the framework of $\alpha\alpha N\Lambda$ four-body cluster model. It is reasonable to employ $\alpha\alpha N\Lambda$ four-body model, since the core nuclei ^{9}B and ^{9}Be are well described by using $\alpha\alpha N$ three-body cluster model, and, therefore, it should be possible to model the structure change of ^{9}B and ^{9}Be due to the addition of one Λ particle as four-body problem.

Another interesting insight is related to the charge symmetry breaking (CSB) components in the ΛN interaction. It is considered that the most reliable evidence for CSB appears in the Λ binding energies B_Λ of the $A = 4$ members with $T = 1/2$ (${}^4_{\Lambda}$He and ${}^4_{\Lambda}$H). Then, the CSB effects are attributed to the differences $\Delta_{CSB} = B_\Lambda({}^4_{\Lambda}\mathrm{He}) - B_\Lambda({}^4_{\Lambda}\mathrm{H})$, the experimental values of which are 0.35 ± 0.06 MeV and 0.24 ± 0.06 MeV for the ground (0^+) and excited (1^+) states, respectively.

The pioneering idea for the origin of the CSB interaction was given in Ref. 7), where Λ-Σ^0 mixing leads to an OPEP-type CSB interaction. This type of meson-theoretical CSB model was shown yield a Δ_{CSB} value for the 0^+ state in ${}^4_{\Lambda}$He and ${}^4_{\Lambda}$H more or less consistent with to the experimental value. Such interactions, however, could not reproduce the Δ_{CSB} value for the 1^+ state.[9),10)]

The CSB effect is generated also by treating the masses of $\Sigma^{\pm,0}$ explicitly in $(NNN\Lambda)$+$(NNN\Sigma)$ coupled four-body calculations of ${}^4_{\Lambda}$He and ${}^4_{\Lambda}$H. In modern YN interactions such as the NSC models[12),13)] both elements of the Λ-Σ^0 mixing and the mass difference of $\Sigma^{\pm,0}$ are taken into account. The exact four-body calculations for ${}^4_{\Lambda}$He and ${}^4_{\Lambda}$H were performed using NSC89/97e models in Ref. 11). It was shown here that the CSB effect was brought about dominantly by the $\Sigma^{\pm,0}$ mass-difference effect. The calculated value of Δ_{CSB} in the 0^+ state was rather smaller than (in good agreement with) the experimental value for NSC97e (NSC89). In case of the 1^+

states, the Δ_{CSB} value for NSC97e had the opposite sign from the observed value, and there appeared no bound state for NSC89.

Thus, the origin of the CSB effect in ${}^{4}_{\Lambda}$He and ${}^{4}_{\Lambda}$H is still an open question.

As an another approach, phenomenological central CSB interactions were introduced in Refs. 8) 10) so as to reproduce the Δ_{CSB} values apart from the origin of the CSB effect. Our present work is along this line: we introduce a phenomenological central CSB interaction so as to reproduce the Δ_{CSB} values of ${}^{4}_{\Lambda}$H and ${}^{4}_{\Lambda}$He, and use this CSB interaction in order to investigate the CSB effects in heavier systems. There exist mirror hypernuclei in the p-shell region such as the $A = 7$, $T = 1$ multiplet (${}^{7}_{\Lambda}$He, ${}^{7}_{\Lambda}$Li*, ${}^{7}_{\Lambda}$Be), $A = 8$, $T = 1/2$ multiplet (${}^{8}_{\Lambda}$Li, ${}^{8}_{\Lambda}$Be), $A = 10$, $T = 1/2$ multiplet (${}^{10}_{\Lambda}$Be, ${}^{10}_{\Lambda}$B), and so on. Historically, some authors mentioned CSB effects in these p-shell Λ hypernuclei.[14),15)]

In the past, accurate estimates of CSB effects in the p-shell region have been of limited consideration, because the Coulomb-energies contribute far more than the CSB interaction:[15)] There has been no microscopic calculation of these hypernuclei taking account of the CSB interaction. Recently, in Ref. 3), we studied for the first time the CSB effects in ${}^{7}_{\Lambda}$He, ${}^{7}_{\Lambda}$Li and ${}^{7}_{\Lambda}$Be within the $\alpha + \Lambda + N + N$ four-body model, and those in ${}^{8}_{\Lambda}$Li and ${}^{8}_{\Lambda}$Be within the $\alpha + t({}^{3}\mathrm{He})+\Lambda$ three-body model using the phenomenological even-state CSB interaction determined in ${}^{4}_{\Lambda}$He and ${}^{4}_{\Lambda}$H. This CSB interaction leads to be inconsistent with the observed data for ${}^{8}_{\Lambda}$Li and ${}^{8}_{\Lambda}$Be. Then, as a trial, we introduced an odd-state component of the CSB interaction with opposite sign to the even-state CSB so as to reproduce the observed binding energies of ${}^{8}_{\Lambda}$Li and ${}^{8}_{\Lambda}$Be. It is likely that this odd-state CSB interaction contributes to binding energies of $A = 7$ and 10 Λ hypernuclei as long as we use the even-state CSB interaction to reproduce the observed binding energies of $A = 4$ hypernuclei. Recently, a new experimental data for ${}^{7}_{\Lambda}$He by $(e, e'K^{+})$ were reported at Thomas Jefferson National Accelerator Facility (JLab).[16)]

In this work, we study $A = 10$ hypernuclei within the framework of an $\alpha + \alpha + N + \Lambda$ four-body model so as to take account of the full correlations among all the constituent sub-units. Two-body interactions among constituent units are chosen so as to reproduce all the existing binding energies of the sub-systems ($\alpha N, \alpha\alpha\Lambda, \alpha\Lambda$, and so on). The analysis is performed systematically for ground and excited states of the $\alpha\alpha N\Lambda$ systems with no more adjustable parameters in this stage, so that these predictions offer important guidance for the interpretation of the upcoming hypernucleus experiments such as the ${}^{10}\mathrm{B}(e, e'K^{+})$ ${}^{10}_{\Lambda}$Be reaction at JLab. The CSB effects in binding energies of ${}^{10}_{\Lambda}$B and ${}^{10}_{\Lambda}$Be are investigated in our four-body model using the even-state CSB interaction determined in ${}^{4}_{\Lambda}$He and ${}^{4}_{\Lambda}$H. Furthermore, we introduce trially an odd-state CSB interaction with opposite sign to the even-state CSB part so as to reproduce data of $A = 7$ hypernuclei, and apply it to the present A=10 systems.

In Sec. 2, the microscopic $\alpha\alpha\Lambda N$ calculation method is described. In Sec.3, the interactions are explained. The calculated results and the discussion are presented in Sec.4. Sec. 5 is devoted to a discussion of charge symmetry breaking effects obtained for the $A = 10$ systems. The summary is given in Sec. 6.

§2. Four-body cluster model and method

In this work, the hypernuclei, ${}^{10}_{\Lambda}$B and ${}^{10}_{\Lambda}$Be are considered to be composed of two α clusters, a Λ particle, and a nucleon. The core α clusters are considered to be an inert core and to have the $(0s)^4$ configuration, $\Psi(\alpha)$. The Pauli principle between the valence nucleon and the nucleons in α clusters is taken into account by the orthogonality condition model (OCM),[18] as the valence nucleon's wave function should be orthogonal to nucleons in the α cluster.

Nine sets of Jacobian coordinates for the four-body system of ${}^{10}_{\Lambda}$B and ${}^{10}_{\Lambda}$Be are illustrated in Fig. 1, in which we further take into account the symmetrization between the two αs.

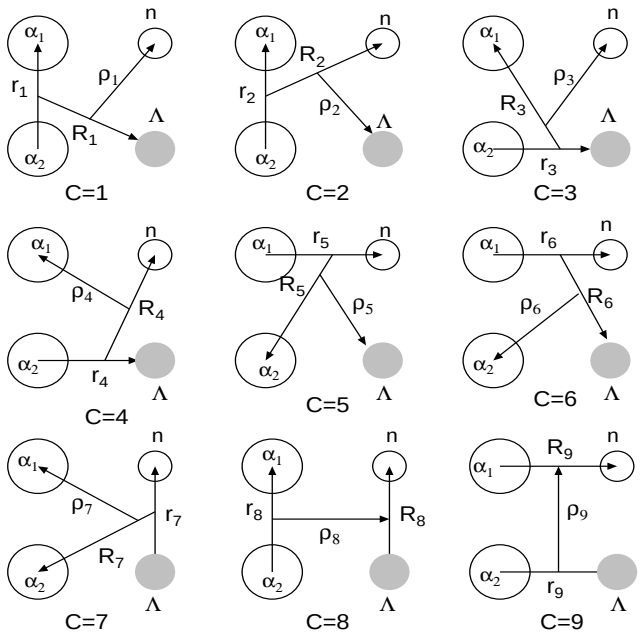

Fig. 1. Jacobi coordinates for all the rearrangement channels ($c = 1 \sim 9$) of the $\alpha + \alpha + \Lambda + N$ four-body system. Two α clusters are to be symmetrized.

The total Hamiltonian and the Schrödinger equation are given by

$$(H - E)\,\Psi_{JM}({}^{10}_{\Lambda}\mathrm{Z}) = 0\ , \tag{2·1}$$

$$H = T + \sum_{a,b} V_{ab} + V_{\mathrm{Pauli}}\ , \tag{2·2}$$

where T is the kinetic-energy operator and V_{ab} is the interaction between constituent particles a and b. The OCM projection operator V_{Pauli} will be given below. The total wavefunction is described as a sum of amplitudes of the rearrangement channels

($c = 1 \sim$ and 9) of Fig. 1 in the LS coupling scheme:

$$\begin{aligned}\Psi_{JM}({}^{10}_{\Lambda}\mathrm{Z}) = &\sum_{c=1}^{9}\sum_{n,N,\nu}\sum_{l,L,\lambda}\sum_{s,I,K} C^{(c)}_{nlNL\nu\lambda SIK} \\ &\times \mathcal{S}_\alpha\Big[\Phi(\alpha_1)\Phi(\alpha_2)\big[\chi_{\frac{1}{2}}(n)\chi_{\frac{1}{2}}(\Lambda)\big]_s \\ &\times \big[\big[\phi^{(c)}_{nl}(\mathbf{r}_c)\psi^{(c)}_{NL}(\mathbf{R}_c)\big]_I \xi^{(c)}_{\nu\lambda}(\boldsymbol{\rho}_c)\big]_K\Big]_{JM} . \end{aligned} \tag{2·3}$$

Here the operator $\mathcal{S}_\alpha$ stands for symmetrization between the two α clusters. $\chi_{\frac{1}{2}}(\Lambda)$ and $\chi_{\frac{1}{2}}(N)$ are the spin functions of the Λ and nucleon, respectively.

Following the Gaussian Expansion Method (GEM),[19),20),1)] we take the functional forms of $\phi_{nlm}(\mathbf{r})$, $\psi_{NLM}(\mathbf{R})$ and $\xi^{(c)}_{\nu\lambda\mu}(\boldsymbol{\rho}_c)$ as

$$\begin{aligned}\phi_{nlm}(\mathbf{r}) &= r^l\, e^{-(r/r_n)^2} Y_{lm}(\widehat{\mathbf{r}}) , \\ \psi_{NLM}(\mathbf{R}) &= R^L\, e^{-(R/R_N)^2} Y_{LM}(\widehat{\mathbf{R}}) , \\ \xi_{\nu\lambda\mu}(\boldsymbol{\rho}) &= \rho^\lambda\, e^{-(\rho/\rho_\nu)^2} Y_{\lambda\mu}(\widehat{\boldsymbol{\rho}}) , \end{aligned} \tag{2·4}$$

where the Gaussian range parameters are chosen according to geometrical progressions:

$$\begin{aligned} r_n &= r_1 a^{n-1} \qquad (n = 1 - n_{\max}) , \\ R_N &= R_1 A^{N-1} \quad (N = 1 - N_{\max}) , \\ \rho_\nu &= \rho_1 \alpha^{\nu-1} \qquad (\nu = 1 - \nu_{\max}) . \end{aligned} \tag{2·5}$$

The eigenenergy E in Eq.(2.1) and the coefficients C in Eq.(2.3) are determined by the Rayleigh-Ritz variational method.

The Pauli principle between nucleons belonging to two α clusters is taken into account by the orthogonality condition model (OCM).[18)] The OCM projection operator V_{Pauli} appearing in Eq. (2.2) is represented by

$$V_{\mathrm{Pauli}} = \lim_{\gamma\to\infty}\ \gamma\ \sum_f |\phi_f(\mathbf{r}_{\alpha x})\rangle\langle\phi_f(\mathbf{r}'_{\alpha x})| , \tag{2·6}$$

which rules out the amplitude of the Pauli-forbidden $\alpha-\alpha$ and α-n relative states $\phi_f(\mathbf{r}_{\alpha x})$ from the four-body total wavefunction.[21)] The forbidden states are $f = 0S, 1S, 0D$ for $x = \alpha$ and $f = 0S$ for $x = n$, respectively. The Gaussian range parameter b of the single-particle $0s$ orbit in the α cluster $(0s)^4$ is taken to be $b = 1.358$ fm so as to reproduce the size of the α cluster. In the actual calculations, the strength γ for V_{Pauli} is taken to be 10^4 MeV, which is large enough to push the unphysical forbidden state to the very high energy region, while keeping the physical states unchanged.

§3. Interactions

3.1. *Charge symmetry parts*

For $V_{N\alpha}$, we employ the effective potential proposed in Ref.22), which is designed so as to reproduce well low-energy scattering phase shifts of the αN system. The Pauli principle between nucleons belonging to the α and the valence nucleon is taken into account by the orthogonality condition model (OCM)[18] as mentioned before.

For $V_{\Lambda N}$, we employ the same as used in the structure calculations of $A = 7$ hypernuclei in Refs.3), 25). Namely, this is an effective single-channel interaction simulating the basic features of the Nijmegen model NSC97f,[13] where the ΛN-ΣN coupling effects are renormalized into ΛN-ΛN parts: We use three-range Gaussian potentials designed to reproduce the ΛN scattering phase shifts calculated from NSC97f, with their second-range strengths in the ${}^3E$ and ${}^1E$ states adjusted so that the calculated energies of the 0^+-1^+ doublet state in the $NNN\Lambda$ four-body system chosen to reproduce the observed splittings of ${}^4_\Lambda$H. Furthermore, the spin-spin parts in the odd states are tuned to yield the experimental values of the splitting energies of ${}^7_\Lambda$Li. The symmetric LS (SLS) and anti-symmetric LS (ALS) parts in $V_{\Lambda N}$ are chosen so as to be consistent with the ${}^9_\Lambda$Be data: The SLS and ALS parts derived from NSC97f with the G-matrix procedure are represented in the two-range form, and then the ALS part is enhanced so as to reproduce the measured $5/2^+$-$3/2^+$ splitting energy in the $2\alpha + \Lambda$ cluster model.[2]

The interaction $V_{\alpha\Lambda}$ is obtained by folding the ΛN G-matrix interaction derived from the Nijmegen model F(NF)[23] with the density of the α cluster,[24] its strength being adjusted so as to reproduce the experimental value of $B_\Lambda({}^5_\Lambda\mathrm{He})$. Furthermore, we use $\alpha\Lambda$ SLS and ALS terms which are obtained by folding the same ΛN SLS and ALS parts as mentioned before.

For $V_{\alpha\alpha}$, we employ the potential that has been used often in the OCM-based cluster-model study of light nuclei.[26] The potential reproduces reasonably well the low-energy scattering phase shifts of the $\alpha\alpha$ system. The Coulomb potentials are constructed by folding the *p*-*p* Coulomb force with the proton densities of all the participating clusters. Since the use of the present $\alpha\alpha$ and αn interactions does not precisely reproduce the energies of the low-lying states of ^{9}Be as measured from the $\alpha\alpha n$ threshold, we introduce an additional phenomenological $\alpha\alpha n$ three-body force so as to fit the observed energies of the $3/2^-_1$ ground state and $5/2^-_1$, $1/2^-_1$ and $1/2^+_1$ excited states in ^{9}Be. The parameters of this $\alpha\alpha n$ three-body force are listed in Ref.27). This $V_{\alpha\alpha}$ potential is applied to the three-body calculation of the $\alpha\alpha p$ system, and the energy of the ground state reproduces the observed data well.

3.2. *Charge symmetry breaking interaction*

It is beyond the scope in this work to explore the origin of the CSB interaction. We employ here the following phenomenological CSB interaction with one-range Gaussian form :

$$V^{\mathrm{CSB}}_{\Lambda N}(r) = -\frac{\tau_z}{2}\Big[\frac{1+P_r}{2}(v_0^{\mathrm{even,CSB}} + \boldsymbol{\sigma}_\Lambda\cdot\boldsymbol{\sigma}_N v^{\mathrm{even,CSB}}_{\sigma_\Lambda\cdot\sigma_N})\, e^{-\beta_{\mathrm{even}}\, r^2}$$

$$+\frac{1-P_r}{2}(v_0^{\rm odd,CSB}+\boldsymbol{\sigma}_\Lambda\cdot\boldsymbol{\sigma}_N v_{\sigma_\Lambda\cdot\sigma_N}^{\rm odd,CSB})\,e^{-\beta_{\rm odd}\,r^2}\Big], \tag{3·1}$$

which includes spin-independent and spin-spin parts. The range parameter, $\beta_{\rm even}$ is taken to be 1.0 fm^{-2}. The parameters $v_0^{\rm even}$ and $v_{\sigma\sigma}^{\rm even}$ are determined phenomenologically so as to reproduce the values of Δ_{CSB} derived from the Λ binding energies of the 0^+ and 1^+ states in the four-body calculation of ${}^4_\Lambda$H (${}^4_\Lambda$He). Then, we obtain $v_0^{\rm even,CSB}=8.0$ MeV and $v_{\sigma\sigma}^{\rm even,CSB}$=0.7 MeV.

In order to extract the information about the odd-state part of CSB, it is necessary to study iso-multiplet hypernuclei in the p-shell region. A suitable system for such a study is ${}^7_\Lambda$He, in which the core nucleus ^{6}He is in a bound state. The JLab E01-011 experiment measured ^{7}Li $(e,e'K^+)^7_\Lambda$He reaction and reported the binding energy of ${}^7_\Lambda$He ground state to be $5.68\pm0.03\pm0.25$ MeV for the first time.[16),17)] The present experimental data has a large systematic error which is the same order to the discussing CSB effect. They measured the same reaction with the improved calibration in the JLab E05-115 experiment[28)] and more accurate result will be obtained in near future. Before the final experimental result of result of ${}^7_\Lambda$He is obtained, we will use our calculated binding energy of ${}^7_\Lambda$He, $B_\Lambda=5.36$ MeV which locates around the limit of the current experimental error, to tune the strength and range of the odd-state. The range parameter, $\beta_{\rm odd}$ is taken to be 1.5 fm. The strengths , $v_0^{\rm odd,CSB}$, $v_{\sigma\sigma}^{\rm odd,CSB}$ are taken to be 16.0 MeV and 0.7 MeV, respectively. Using these potential parameters, the Λ-separation energy of the mirror Λ hypernucleus, ${}^7_\Lambda$Be is 5.27 MeV, which reproduces the observed data, too.

§4. Results

4.1. *spin doublet states of $A=10$ hypernuclei*

First, let us describe the level structures of ${}^{10}_\Lambda$B and ${}^{10}_\Lambda$Be obtained with the $\alpha+\Lambda+N+N$ four-body model, when the CSB interaction is not included. Calculations are performed for four-body bound states in these Λ hypernuclei.

In Figs. 2 and 3 and in Table I, we show the level structures of ${}^{10}_\Lambda$B and ${}^{10}_\Lambda$Be. In each figure, hypernuclear levels are shown in four columns in order to demonstrate separately the effects of the even-state and odd-state ΛN interactions, and also the SLS and ALS interactions. Even when the CSB interactions are switched on, their small contributions do not alter the features of these figures. Table I gives calculated values of Λ binding energies and root mean square (r.m.s.) distances of subsystems in ${}^{10}_\Lambda$B and ${}^{10}_\Lambda$Be.

It is considered that the 1^--2^-_1 spin-doublet states in ${}^{10}_\Lambda$B and ${}^{10}_\Lambda$Be, and also the 2^-_2-3^- and 0^+-1^+ spin-doublet states in ${}^{10}_\Lambda$Be, give useful information about the underlying spin-dependence of the ΛN interaction. It should be noted that the ΛN interaction used in the present calculations is identical to the one used in our previous analyses of the $T=0$ spin-doublet state of ${}^7_\Lambda$Li[3)] and the $3/2^+$-$5/2^+$ spin-doublet states of ${}^7_\Lambda$He and ${}^7_\Lambda$Li with $T=1$.[25)] That is no additional parameter for adjusting to the experimental data is used in the present calculations.

As shown in Fig. 2, we see that the resultant energy splitting of the 1^--2^-_1 states

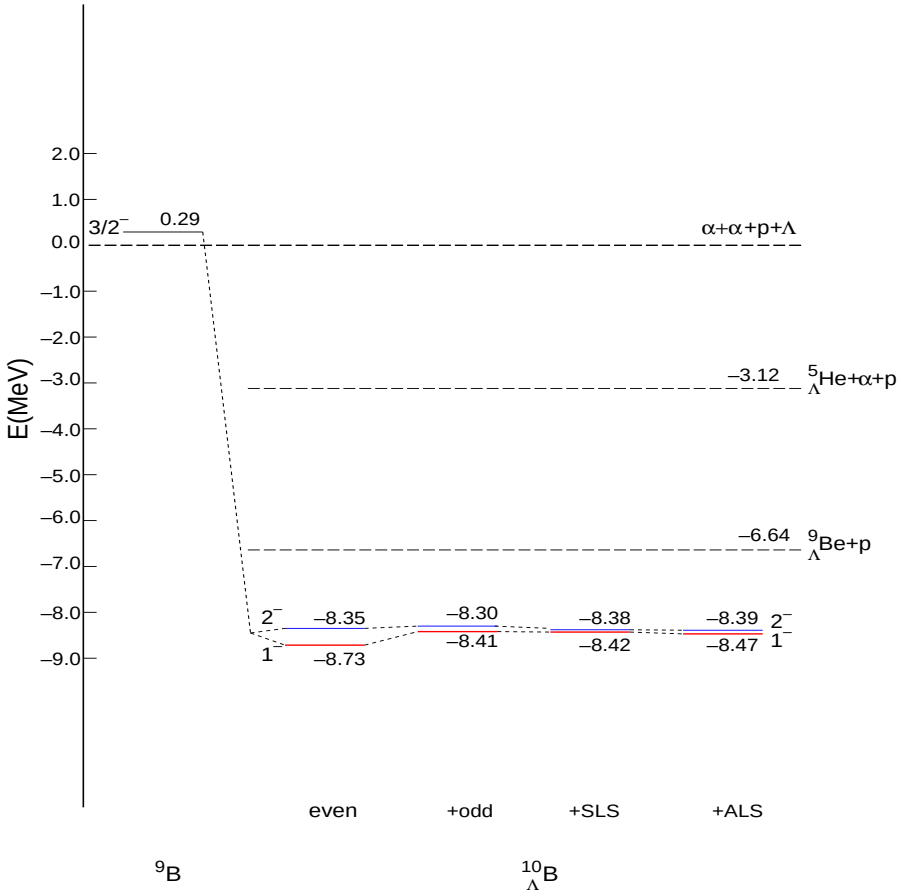

Fig. 2. (color online). Calculated energy levels of ^{9}B and $^{10}_{\Lambda}$B. The charge symmetry breaking potential is not included in $^{10}_{\Lambda}$B. The level energies are measured with respect to $\alpha+\alpha+\Lambda+p$ particle breakup threshold.

in $^{10}_{\Lambda}$B is 0.08 MeV, with combined contributions from the spin-spin, SLS and ALS interactions. For the study of the ΛN spin-dependent interaction, in BNL-E930, they tried to measure the 1^--2^-_1 spin-doublet states in $^{10}_{\Lambda}$B using the ^{10}B$(K^-,\pi^-\gamma)$ reaction. However, the $M1$ transition between the ground-state doublet members $(2^-_1 \to 1^-)$ was not observed. This measurement suggests the following two possibilities: The energy splitting between the 1^- and 2^-_1 states is less than 100 keV and the γ ray cannot be observed, since the γ-ray detection efficiency drops rapidly below 100 keV. The other suggestion is that the 2^-_1 state, which is dominantly produced by the $(K^-,\pi^-\gamma)$ reaction, is the ground state. Our result supports the former.

Next, let us see in more detail how the ΛN spin-spin interactions contribute to the 1^--2^- doublets in $^{10}_{\Lambda}$B. The 1^- state is composed of $[K=1(N\Lambda)_{s=0,1}]_{J=1^-}$ and $[K=2(N\Lambda)_{s=1}]_{J=1^-}$, where the K is the angular momentum and s is the spin of $N-\Lambda$ described in Eq. (2.3). Among these three components, $[K=1(N\Lambda)_{s=0,1}]_{J=1^-}$

components are comparable with each other. On the other hand, the 2_1^- state is composed of $[K = 1(N\Lambda)_{s=1}]_{J=2^-}$ and $[K = 2(N\Lambda)_{s=0,1}]_{J=2_1^-}$ components, where the $[K = 1(N\Lambda)_{s=1}]_{J=2_1^-}$ and $[K = 2(N\Lambda)_{s=1}]_{J=2_1^-}$ components are larger than the other one. The $V_{\Lambda N}(^1E)$ is more attractive than the $V_{\Lambda N}(^3E)$, when they are adjusted so as to reproduce the 0^+-1^+ splitting energy in ${}^4_\Lambda$H (${}^4_\Lambda$He). In ${}^{10}_\Lambda$B, this even-state interaction makes the 1^- state lower than 2_1^- state. The value obtained for the splitting energy is 0.38 MeV. This value is far larger than the above limitation of 100 keV suggested by the no γ-ray observation in BNL-E930. On the other hand, the calculated value of B_Λ in the ground state is 9.02 MeV, which is consistent with the experimental value of 8.89 ± 0.12 MeV within the error bar.

Next, when the odd-state interaction is switched on, the energy splitting is reduced to 0.11 MeV (see "+odd" column). The reason for this reduction is because $V_{\Lambda N}(^1O)$ is more repulsive than $V_{\Lambda N}(^3O)$ as indicated in our analysis for the $1/2^+$-$3/2^+$ spin-doublet state in ${}^7_\Lambda$Li. Then, in ${}^{10}_\Lambda$B, the 1^- state including dominantly the ΛN spin-singlet component is pushed up more than the 2_1^- state.

Moreover, we study the effects of the SLS and ALS interactions on 1^- and 2_1^- doublet states. As shown in Fig.2, the SLS works attractively for the 2_1^- state because the contribution of the ΛN spin-triplet state is dominant in this state, while its contribution is very small to the 1^- state which is dominated by the spin-singlet component. Thus, the 1^--2_1^- splitting is found to be reduced by the SLS.

On the other hand, the ALS works significantly in the 1^- state, because the ALS acts between the spin= 0 and 1 ΛN components and both of them are included in the 1^- state. However, the ALS contribution is not significant in the 2_1^- state, because this state is dominated by the spin =1 ΛN component.

As a result of including both the spin-spin and spin-orbit terms, the energy splitting of the 1^--2_1^- states of ${}^{10}_\Lambda$B leads to be 0.08 MeV. Then, we obtain the calculated value $B_\Lambda({}^{10}_\Lambda\mathrm{B})$=8.76 MeV which does not differ significantly from the experimental value, 8.89 ± 0.12 MeV.

We can see the same tendency in ${}^{10}_\Lambda$Be and the resultant energy splitting is 0.08 MeV, which is the same as that of ${}^{10}_\Lambda$B, as shown in Fig.3. The calculated B_Λ value of the ground state is 8.94 MeV. As in the ${}^{10}_\Lambda$B case, this value is rather close to the experimental value $B_\Lambda({}^{10}_\Lambda\mathrm{Be})$=$9.11 \pm 0.22$ MeV. A more detailed discussion of the binding energies of ${}^{10}_\Lambda$B and ${}^{10}_\Lambda$Be with/without CSB interaction will appear in the next session. Next, let us discuss one more spin-doublet state, 2_2^--3^-, in ${}^{10}_\Lambda$Be. The dominant component of the 2_2^- (3^-) state is $[K = 2(N\Lambda)_{s=0}]_{J=2_2^-}$ ($[K = 2(N\Lambda)_{s=1}]_{J=3^-}$). Then, with the use of our even state interaction, the 2_2^- state is lower than 3^- state and the energy splitting is 0.43 MeV. When the odd state interaction is included in calculations of 2_2^- and 3^- states, the energy of the 2_2^- state is pushed up more than that of the 3^- state due to the repulsive contribution of the $V_{\Lambda N}^{(^1O)}$ component and energy splitting is 0.12 MeV. When the SLS interaction is added to the calculations of these states, the SLS contributes dominantly to the 3^- state. Finally, the repulsive ALS interaction, having the opposite sign of the SLS, contributes mainly to the 2_2^- state including both of spin-singlet and spin-triplet states. As a result, we have 0.05 MeV for the 3^--2_2^- doublet splitting.

Furthermore, the above the 3^- and 2^-_2 states, we have 0^+ and 1^+ states as bound states which is composed of ${}^9\mathrm{Be}(1/2^+) + \Lambda(0s_{1/2})$. In the core nucleus, ^{9}Be, the $1/2^+$ state is observed as the first excited state and is lower than the $5/2^-$ and $1/2^-$ excited states, despite the last neutron in this $1/2^+$ state presumably occupying the $1s_{1/2}$ orbit in the simple shell model configuration, whereas the next two excited states with negative parity would have $1p$-shell configurations. It is interesting to see that the order of the 3^-, 2^-_2, 0^+ and 1^+ states is reversed from ^{9}Be to ${}^{10}_{\Lambda}$Be. The $5/2^-$ state is composed of ${}^8\mathrm{Be}(2^+) + n(p_{1/2}, p3/2)$ and then there is a centrifugal barrier between $\alpha\alpha$ and a valence neutron, while the $1/2^+$ state does not have any barrier. Thus it is considered that the $5/2^-$ state is more compact than the $1/2^+$ state. When a Λ particle adds into these states, we see the energy gain is larger than in the compactly coupled state ($5/2^-$) than in the loosely coupled state ($1/2^+$). It should be noted that the same type of theoretical prediction was reported in our early work[2] for the $\alpha\alpha\alpha\Lambda$ four-body model of ${}^{13}_{\Lambda}$C, where the Λ particle is added to the compact bound state (3^-_1) and to the loosely bound state (0^+_2) in ^{12}C.

Let us discuss about energy splitting of this positive parity states. The dominant component of the 0^+ (1^+) is $[K = 0(N\Lambda)_{s=0}]_{0^+}$ ($[K = 0(N\Lambda)_{s=1}]_{1^+}$). Then using the even state spin-spin interaction, the 0^+ state is lower than the 1^+ state and energy splitting is 0.57 MeV. When the odd state spin-spin interaction is employed, the energy of the 0^+ is pushed up more than that of the 1^+ state due to the repulsive contribution of the $V^{(^1O)}_{\Lambda N}$ component and the energy splitting is 0.26MeV. Since these two states are composed of ${}^9\mathrm{Be}(1/2^+) + \Lambda(0s_{1/2})$ as mentioned before, then the relative angular momenta between composed particles are almost s-wave, then spin-orbit contribution for these doublets is very small. As shown in Fig.3, we see that the contributions of SLS and ALS for these doublets are small. Thus, we have 0.2 MeV finally for this positive parity doublet.

In Fig.3, we found that the energy splittings of the negative parity doublets are less than 0.1 MeV, while that of the positive parity state is much larger. The reason is as follows: The αN spin-orbit interaction makes 2^- state lower than the 1^- state. On the other hand, the ΛN spin-spin interaction makes 1^- state lower than the 2^- state. Due to the cancellation between αN spin-orbit interaction and ΛN spin-spin interaction, we have less than 0.1 MeV splitting energy. In order to investigate the efect of the αN spin-orbit interaction for the 1^--2^- doublet state, as a trial, we turn off the αN spin-orbit term. In this case, we use ΛN even and odd-state spin-spin forces. Then, the energy splitting is obtained to be 0.27 MeV owing to the even- and odd-state spin-spin forces. This value is similar with one of 0^+-1^+ state. Thus, we find that αN spin-orbit force give a contribution to the energy splitting of the ground state doublet.

On the other hand, in the case of 0^+ and 1^+ states, the αN spin-orbit contribution to this energy splitting is significantly small, because composed particles α and N are in the s-state relatively. As a result, we get the pure contribution of the spin-spin ΛN interaction for the energy splitting of 0^+ and 1^+ states, 0.2 MeV.

Then, it would be difficult to observe γ-ray transitions between the negative parity spin-doublet partners, but it might be possible to observed γ-ray from 0^+ and

1^+ states.

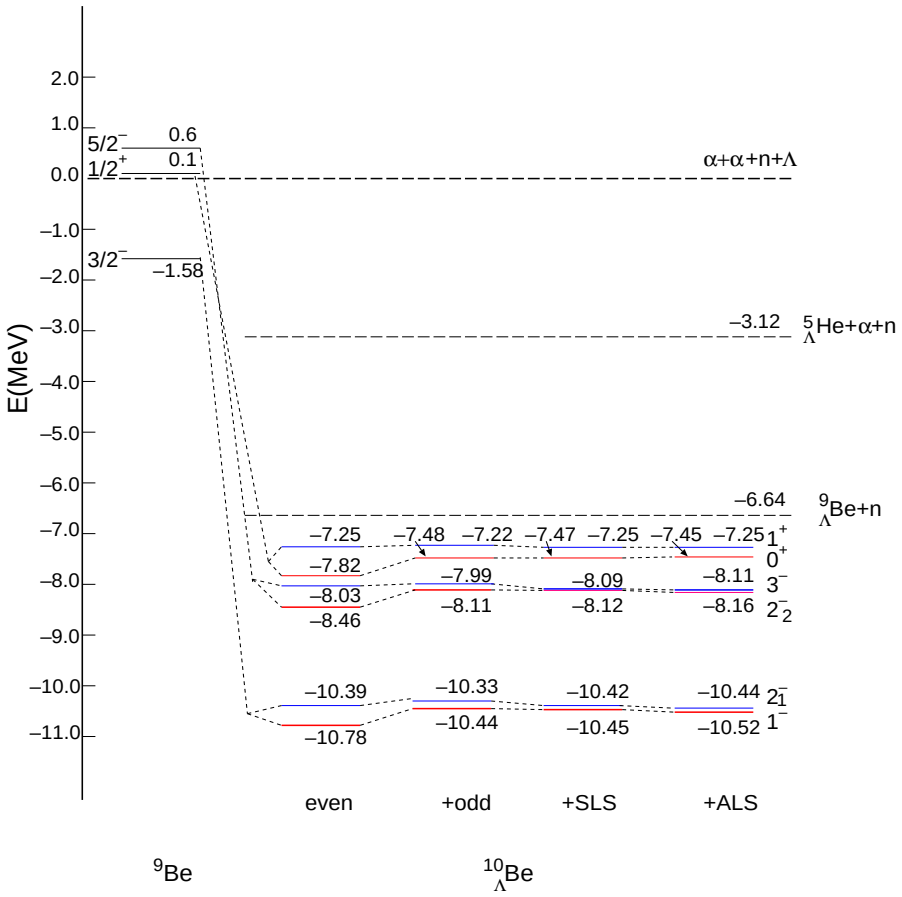

Fig. 3. (color online). Calculated energy levels of ^{9}Be and $^{10}_{\Lambda}$Be. The charge symmetry breaking potential is not included in $^{10}_{\Lambda}$Be. The level energies are measured with respect to $\alpha+\alpha+\Lambda+n$ particle breakup threshold.

It is interesting to explore the glue-like role of the Λ particle in $^{10}_{\Lambda}$B and $^{10}_{\Lambda}$Be. Though the ground state of ^{9}B is unbound, the corresponding states $(1^-, 2^-_1)$ in Λ hypernuleus becomes bound by 1.7 $\sim$ 2.0 MeV due to the addition of a Λ. On the other hand, the ground state of the core nucleus ^{9}Be is bound by 1.58 MeV with respect to the $\alpha+\alpha+n$ three-body threshold. Owing to an additional Λ particle, the corresponding ground state of $^{10}_{\Lambda}$Be become rather deeply bound, by $\sim$ 4 MeV. Furthermore, the $5/2^-$ resonant state of ^{9}Be become bound (3^- and 2^-_2 in $^{10}_{\Lambda}$Be) by $\sim$ 1.2 MeV due to the presence of the Λ particle. In addition, when a Λ particle is added to the $1/2^+$ state of ^{9}Be, the 0^+ and 1^+ states of $^{10}_{\Lambda}$Be become weakly bound by less than 1.0 MeV.

In Table I, we list the calculated values of the r.m.s. radii between composed particles, $\bar{r}_{\alpha-\alpha}$, $\bar{r}_{\alpha-\Lambda}$, $\bar{r}_{\alpha-N}$ and $\bar{r}_{\Lambda-N}$ in our four-body model of $^{10}_{\Lambda}$B and $^{10}_{\Lambda}$Be.

Table I. Calculated energies of the low-lying states of (a) ${}^{10}_{\Lambda}$B and (b)${}^{10}_{\Lambda}$Be without the charge symmetry breaking potential, together with those of the corresponding states of ^{9}B and ^{9}Be , respectively. E stands for the total interaction energy among constituent particles. The energies in the parentheses are measured from the corresponding lowest particle-decay thresholds ${}^{9}_{\Lambda}$Be+ N for ${}^{10}_{\Lambda}$B and ${}^{10}_{\Lambda}$Be. The calculated r.m.s. distances, $\bar{r}_{\alpha-\alpha}$, $\bar{r}_{\alpha-\Lambda}$ $\bar{r}_{\alpha-n}$, $\bar{r}_{\Lambda-N}$ are also listed for the bound state.

(a)

	^{9}B($\alpha\alpha p$)	${}^{10}_{\Lambda}$B($\alpha\alpha\Lambda p$)	
J^π	$3/2^-$	1^-	2^-
E (MeV)	$+0.29$	-8.47	-8.39
$E^{\rm exp}$(MeV)	0.28		
		(-1.83)	(-1.75)
B_Λ(MeV)		8.76	8.67
$B_\Lambda^{\rm exp}$ (MeV)		8.89 ± 0.12	
$\bar{r}_{\alpha-\alpha}$(fm)		3.32	3.30
$\bar{r}_{\alpha-\Lambda}$(fm)		3.04	3.02
$\bar{r}_{\alpha-p}$(fm)		3.64	3.64
$\bar{r}_{\Lambda-p}$(fm)		3.86	3.87

(b)

	^{9}Be($\alpha\alpha n$)		${}^{10}_{\Lambda}$Be($\alpha\alpha\Lambda n$)					
J^π	$3/2^-$	$5/2^-$	1^-	2^-_1	2^-_2	3^-	0^+	1^+
E (MeV)	-1.58	0.60	-10.42	-10.38	-8.13	-8.01	-7.45	-7.25
$E^{\rm exp}$(MeV)	-1.58	0.85						
			(-3.76)	(-3.74)	(-1.47)	(-1.35)	(-0.81)	(-0.61)
B_Λ(MeV)			8.84	8.80	6.63	6.26	5.87	5.67
$B_\Lambda^{\rm exp}$ (MeV)			9.11 ± 0.22					
$\bar{r}_{\alpha-\alpha}$(fm)	3.68	-	3.27	3.26	3.29	3.24	3.78	3.76
$\bar{r}_{\alpha-\Lambda}$(fm)			3.02	3.00	3.02	3.00	3.31	3.30
$\bar{r}_{\alpha-n}$(fm)	4.56	-	3.52	3.51	3.56	3.56	4.95	5.04
$\bar{r}_{\Lambda-n}$(fm)			3.77	3.75	3.85	3.80	5.04	5.15

From the calculated rms radii, it is interesting to look at the dynamical change of the nuclear core ^{9}Be, which occurs due to the addition of a Λ particle. The possibility of nuclear-core shrinkage due to a addition of Λ-particle was originally pointed out in Ref. 29) by using the $\alpha x \Lambda$ three-cluster model ($x = n, p, d, t,{}^{3}$He, and α) for p-shell Λ hypernuclei. As for the hypernucleus ${}^{7}_{\Lambda}$Li, the prediction of some 20 % shrinkage, in Ref. 29) and in an updated calculation,[30] was confirmed by experiment.[31] As shown in Table I, the rms distance $\bar{r}_{\alpha-\alpha}$ between two α clusters, and $\bar{r}_{\alpha-N}$ between α and nucleon, are reduced by $12-17$ % with the addition of a Λ particle.

As shown in Table I, the values of $\bar{r}_{\alpha-N}$ in these systems are larger than those of $\bar{r}_{\alpha-\Lambda}$, indicating that the distributions of valence nucleons have longer-ranged tails than those of the Λ's in the respective systems. Especially, $\bar{r}_{\alpha-N}$ in the 0^+ and the 1^+ states are much larger, around 5 fm than those of the other states. Then, it is expected that these positive parity states have neutron halos.

In order to see the structure of these systems visually, in Fig. 4, we draw the density distributions of the Λ (dashed curve) and valence neutrons (solid curve) of

0^+ state of ${}^{10}_{\Lambda}$Be. For comparison here, also a single-nucleon density in the α core is shown by the dotted curve. You find that we have long-range neutron density as shown in Fig.4.

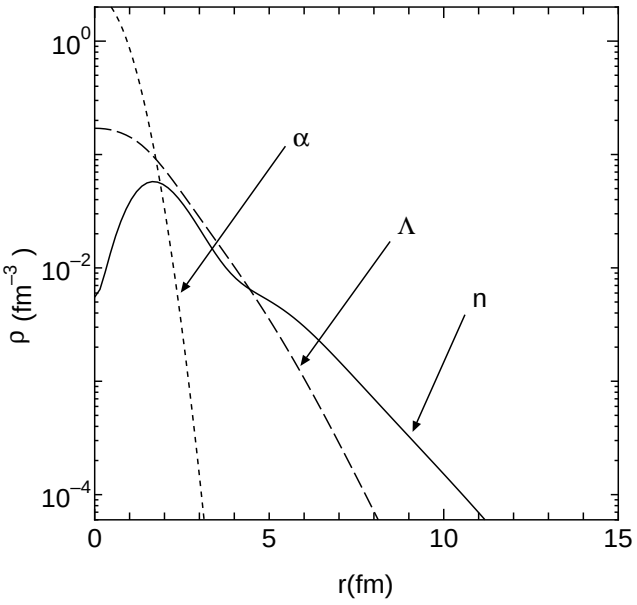

Fig. 4. Calculated density distribution of α, a Λ and a valence nucleon for 0^+ state of ${}^{10}_{\Lambda}$Be without a charge symmetry breaking potential.

In addition, we show the density distributions of 1^- state of ${}^{10}_{\Lambda}$Be and ${}^{10}_{\Lambda}$B in Fig.5. In each case, the density distribution of the Λ has a shorter-ranged tail than that of a valence nucleon, but is extended significantly far away from the α core, which can be thought of as three layers of matter composed of two α clusters, a Λ , and a nucleon.

4.2. *Charge Symmetry breaking effects*

Let us focus on the ground states in ${}^{10}_{\Lambda}$Be and ${}^{10}_{\Lambda}$B. It is likely that the CSB interaction affect in binding energies of these isodoublet hypernuclei.

In subsec.3.2, we introduce the phenomenological CSB potential with the central-force component only. The CS part of the two-body ΛN interaction is fixed to reproduce the averaged energy spectra of ${}^{4}_{\Lambda}$H and ${}^{4}_{\Lambda}$He, and then the even-state part of the CSB interaction is adjusted so as to reproduce both the energy levels of these hypernuclei. In our previous work,[25] this CSB interaction was applied to calculations of the binding energies of the $A = 7$ isotriplet hypernuclei, ${}^{7}_{\Lambda}$He, ${}^{7}_{\Lambda}$Li($T = 1$), and ${}^{7}_{\Lambda}$Be. Here, the CSB interaction works repulsively (+0.20 MeV) and attractively (−0.20 MeV), respectively, in ${}^{7}_{\Lambda}$He and ${}^{7}_{\Lambda}$Be. As a result, our calculated values do not reproduce the observed B_Λs of ${}^{7}_{\Lambda}$He and ${}^{7}_{\Lambda}$Be. Furthermore, in Ref. 25), we pointed out that the same phenomena was seen in the energy difference of the $T = 1/2$ isodoublet $A = 8$ hypernuclei (${}^{8}_{\Lambda}$Li, ${}^{8}_{\Lambda}$Be): The agreement to the observed data of the energy difference becomes worse by introducing the CSB $\Lambda - t({}^3\mathrm{He})$

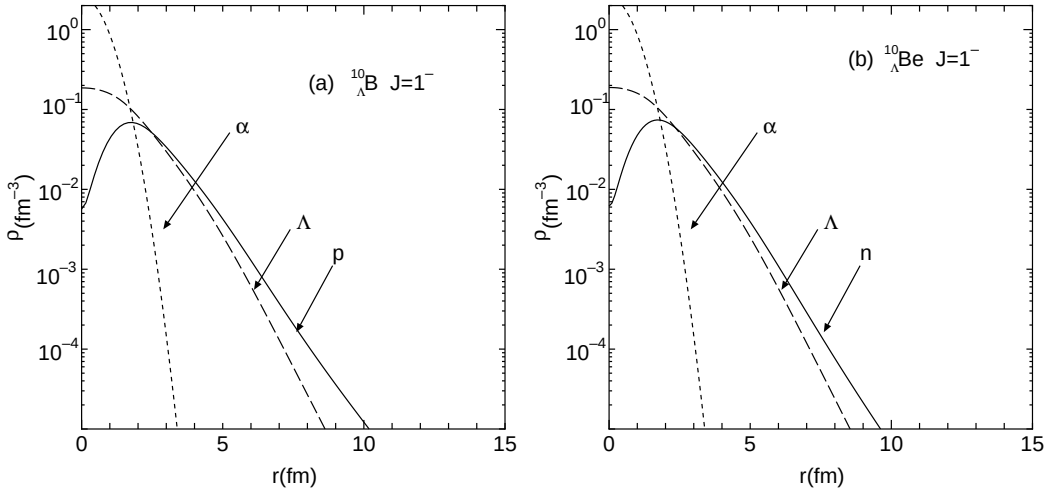

Fig. 5. Calculated density distribution of α, a Λ and a valence nucleon for (a)$^{10}_{\Lambda}$B and (b)$^{10}_{\Lambda}$Be without a charge symmetry breaking potential.

interaction.

Let us discuss the energy difference of $^{10}_{\Lambda}$Be and $^{10}_{\Lambda}$B using even-state CSB interaction employed in $A = 7$ hypernuclei.

First, in Fig. 6(a), we show the energy spectra of the $A = 10$ hypernuclei calculated without a CSB interaction. The calculated B_Λ values of $^{10}_{\Lambda}$Be and $^{10}_{\Lambda}$B are 8.94 and 8.76 MeV, respectively.

Second, we turn on the even-state CSB interaction. In Fig. 6(b), it is found that the CSB interaction works repulsively by +0.1 MeV and attractively by −0.1 MeV in $^{10}_{\Lambda}$Be and $^{10}_{\Lambda}$B, respectively. This behavior is similar to the case of $A = 4$ and 7 hypernuclei.

Let us consider the energies of these $A = 10$ hypernuclei more in detail. In the case of $^{10}_{\Lambda}$Be, the CSB interaction between the Λ and a valence neutron works repulsively and the ground-state binding energy leads to $B_\Lambda = 8.83$ MeV, which is less bound by 0.1 MeV than the value without the CSB effect. In $^{10}_{\Lambda}$B, the CSB interaction contributes attractively by 0.1 MeV, and the binding energy of the ground state is $B_\Lambda = 8.85$ MeV, which is close to the experimental data. In order to see the CSB effect in the $A = 10$ hypernuclei more clearly, let us evaluate the difference between the calculated B_Λ values for $^{10}_{\Lambda}$Be and $^{10}_{\Lambda}$B; $\Delta B_\Lambda^{\rm cal} = B_\Lambda^{\rm cal}(^{10}_{\Lambda}{\rm B}) - B_\Lambda^{\rm cal}(^{10}_{\Lambda}{\rm Be}) = -0.18$ MeV without CSB, which is in good agreement with the experimental value, $\Delta B_\Lambda^{\rm exp} = B_\Lambda^{\rm exp}(^{10}_{\Lambda}{\rm B}) - B_\Lambda^{\rm exp}(^{10}_{\Lambda}{\rm Be}) = -0.22 \pm 0.25$ MeV. Switching on the even-state CSB interaction, the value obtained for $\Delta B_\Lambda^{\rm cal} = 0.02$MeV moves away from the central value of the data, −0.22 MeV.

In this way, we find that if we introduce a phenomenological ΛN CSB interaction, the binding energies of $A = 7, 8, 10$ Λ hypernuclei become inconsistent with the observed data.

We can also discuss the CSB effects in s-shell and p-shell Λ hypernuclei from the experimental data. The observed biding energy of $^{4}_{\Lambda}$He is larger by 0.35 MeV

than that of ${}^{4}_{\Lambda}$H. Namely, it seems that $p\Lambda$ interaction is more attractive than $n\Lambda$ interaction by CSB effect. While, the observed binding energies of ${}^{7}_{\Lambda}$He, ${}^{8}_{\Lambda}$Li and ${}^{10}_{\Lambda}$Be are larger than those of ${}^{7}_{\Lambda}$Be, ${}^{8}_{\Lambda}$Be and ${}^{10}_{\Lambda}$B. This means that the $n\Lambda$ interaction is more attractive than the $p\Lambda$ interaction.

One possibility to solve this contradiction is to re-investigate the experimental data, especially those of s-shell Λ hypernuclei, ${}^{4}_{\Lambda}$H, ${}^{4}_{\Lambda}$He. In fact, it is planned to measure the M1 transition from 1^+ state to the 0^+ state in ${}^{4}_{\Lambda}$He at E13 J-PARC project[32] and to measure Λ separation energy of the 0^+ state in ${}^{4}_{\Lambda}$H at Maintz and JLab.

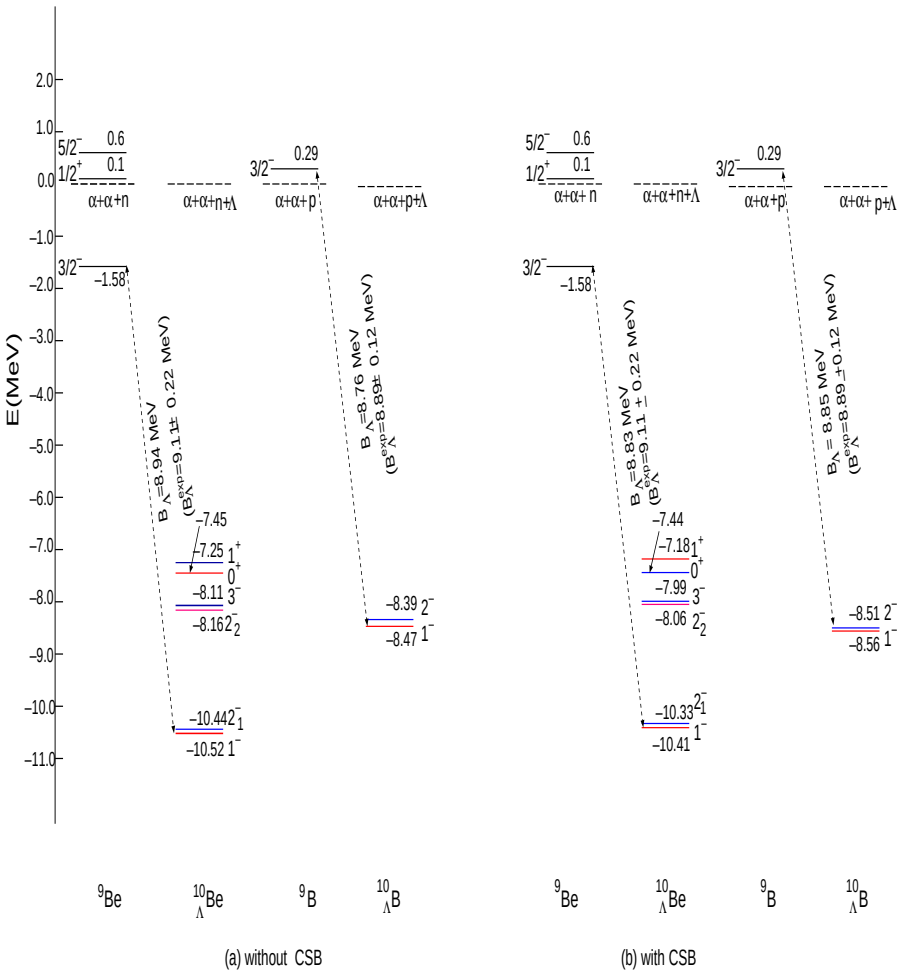

Fig. 6. (color online). Calculated energy levels of ^{9}Be, ${}^{10}_{\Lambda}$Be, ^{9}B, and ${}^{10}_{\Lambda}$B with spin-spin and spin-orbit ΛN interactions. The even-state CSB potential is not included in the calculated energies of ${}^{10}_{\Lambda}$Be and ${}^{10}_{\Lambda}$B of (a), and included in those of (b). The energies are measured from the particle breakup threshold.

One of candidates to solve the contradiction is simply to introduce the odd-state CSB interaction with opposite sign to the even-state CSB interaction. The odd-

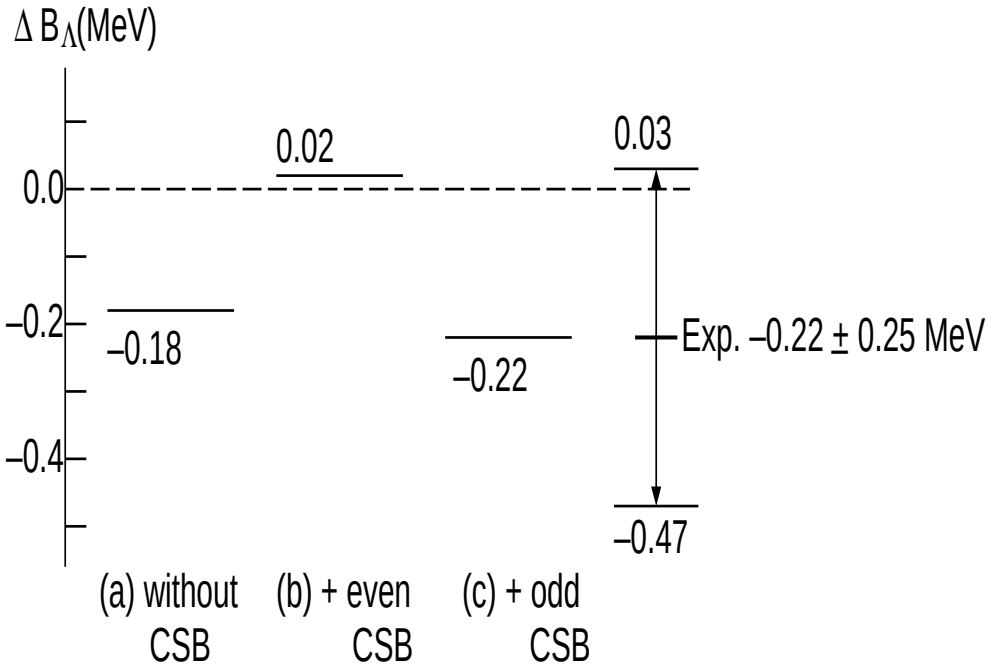

Fig. 7. Calculated energy difference of ${}^{10}_{\Lambda}$Be and ${}^{10}_{\Lambda}$B, $\Delta B_\Lambda({}^{10}_{\Lambda}\mathrm{B}) - B_\Lambda({}^{10}_{\Lambda}\mathrm{Be})$, (a) without CSB, (b) with even-state CSB, and (c) with both even- and odd-state CSB interactions

state CSB interaction is negligible in s-shell Λ hypernuclei but significant in p-shell Λ hypernuclei.

In Ref.25), we pointed out that in order to reproduce the data of these $A = 8$ hyernuclei, it was necessary the odd-state CSB interaction with opposite sign of that of the even state CSB interaction.[25)]

It is expected that such an odd-state CSB interaction plays the same role in the $A = 7$ and 10 hypernuclei. Here, we show the results of ${}^{10}_{\Lambda}$Be and ${}^{10}_{\Lambda}$B without the CSB and with even-state CSB chosen to reproduce the observed binding energies of ${}^{4}_{\Lambda}$H and ${}^{4}_{\Lambda}$He, and with even- and odd-state CSB interactions. The odd-state CSB interaction is introduced with opposite sign to that the even state part, but whose contributions in the ${}^{4}_{\Lambda}$H and ${}^{4}_{\Lambda}$He are negligible. Their potential parameters, strengths and ranges, are fixed so as to reproduce our calculated B_Λ for ${}^{7}_{\Lambda}$He, 5.36 MeV. The detailed potential parameters are mentioned in the subsection 3.2.

Next, we apply the strong odd-state CSB interaction to level structures of ${}^{10}_{\Lambda}$Be and ${}^{10}_{\Lambda}$B. The calculated Λ-separation energies of the 1^- states for ${}^{10}_{\Lambda}$Be and ${}^{10}_{\Lambda}$B are 8.96 MeV and 8.74 MeV, respectively. Then, $\Delta B_\Lambda^{\mathrm{cal}} = -0.22$ MeV, which is in good agreement with $\Delta B_\Lambda^{\mathrm{exp}} = -0.22 \pm 0.25$. The biding energies of $A = 7$ and 10 Λ hypernulclei with and without CSB interaction are listed in Table 2.

Three results of $A = 10$ hypernuclei are summarized in Fig. 7. Three results shown by solid lines are found to be within the experimental error bars. We see deviation by 200 keV in the $\Delta B_\Lambda^{\mathrm{exp}}$ with and without the CSB interaction. Then,

Table II. Calculated Λ separation energies of $A = 7$ and 10 Λ hypernuclei with and without CSB interactions. The $B_\Lambda^{\rm cal}({}^{10}_{\Lambda}{\rm Be}) - B_\Lambda^{\rm cal}({}^{10}_{\Lambda}{\rm B})$ and $\Delta B_\Lambda^{\rm exp} = B_\Lambda^{\rm exp}({}^{10}_{\Lambda}{\rm Be}) - B_\Lambda^{\rm exp}({}^{10}_{\Lambda}{\rm B})$ are listed here.

	without CSB	with even-state CSB	with even+odd-state CSB	Exp.
$B_\Lambda({}^{7}_{\Lambda}{\rm He})$	5.36	5.16	5.36	$5.68 \pm 0.03 \pm 0.25$[16),17)]
$B_\Lambda({}^{7}_{\Lambda}{\rm Li})$	5.28	5.29	5.28	5.26
$B_\Lambda({}^{7}_{\Lambda}{\rm Be})$	5.21	5.44	5.27	5.16±0.08
$B_\Lambda({}^{10}_{\Lambda}{\rm Be})$	8.94	8.83	8.96	9.11 ± 0.22
$B_\Lambda({}^{10}_{\Lambda}{\rm B})$	8.76	8.85	8.74	8.89 ± 0.12
$\Delta B_\Lambda^{\rm cal}$	0.18	−0.02	0.22	0.22 ± 0.25

if high resolution experiments can provide us new data for ${}^{10}_{\Lambda}$Be and ${}^{10}_{\Lambda}$B within 100 keV accuracy in the future , we can obtain information about the CSB interaction.

As shown in Table 2 and Fig.7, the biding energies of $A = 7$ and 10 Λ hypernuclei without CSB interaction reproduce the all data. However, the even-state CSB interaction which reproduce the data of s-shell Λ hypernuclei, ${}^{4}_{\Lambda}$H and ${}^{4}_{\Lambda}$He leads to inconsistency of the biding energies of p-shell Λ hyernuclei. As a trial, then, if we introduce a strong odd-state CSB interaction with opposite sign of even-state CSB interaction, we could reproduce the observed biding energies of $A = 7$ and 10 Λ hypernuclei. However, there still remains a room to discuss the validity of such a strong odd-state CSB interaction. For the CSB effect in light Λ hypernuclei, it is necessary to re-investigate experimental data of s-shell Λ hypernuclei and p-shell Λ hypernuclei as mentioned before. In fact, it is planned to measure the M1 transition from 1^+ state to the 0^+ state in ${}^{4}_{\Lambda}$He at E13 J-PARC project[32)] and to measure Λ separation energy of the 0^+ state in ${}^{4}_{\Lambda}$H at Maintz and JLab. From these measurements, we could conclude whether or not there exist in CSB effect in the binding energies of $A = 4$ hypernuclei. We need wait for these data.

§5. Summary

We study the structure of hypernuclear isodoublet ${}^{10}_{\Lambda}$B and ${}^{10}_{\Lambda}$Be within the framework of $\alpha + \alpha + \Lambda + N$ four-body model. In this model, it is important that all two-body interactions among subunits (two α's, Λ and N) are chosen so as to reproduce the binding energies of all subsystems composed of two and three subunits. The ΛN interaction, which simulates ΛN scattering phase shifts of NSC97f, are adjusted so as to reproduce the observed data for the spin-doublets states, 0^+-1^+ and $1/2^+$-$3/2^+$, of ${}^{4}_{\Lambda}$H and ${}^{7}_{\Lambda}$Li, respectively. Before discussing major conclusion, we comment on our general viewpoint for effective interactions used in our cluster-model analyses. Our basic assumption in this work is that the $\Lambda N - \Sigma N$ coupling interaction can be renormalized into the $\Lambda N - \Lambda N$ interaction effectively. It should be noted that our renormalizations into effective ΛN interactions are made so as to reproduce experimental values of binding energies of subunits such as ΛN, $\Lambda\alpha$, $\Lambda\alpha\alpha$ and so on. Here

we emphasized that the validity of nuclear models and effective interactions in them should be based on the consistency with experimental data: In our cluster-model approach, the experimental data of above hypernuclei are reproduced systematically with use of our effective interactions.

The main conclusions can be summarized as follows:

(1) We calculated spin-doublet states of 1^--2^-_1 in ${}^{10}_{\Lambda}$B whose measurement was obtained in BNL930.[4] The calculated splitting energy is 0.08 MeV. This small value is less than the 0.1 MeV precision for detecting the M1 transition from the 2^- to the 1^- state, which is consistent with the experimental fact of no observed γ-ray. Furthermore, we calculated the spin-doublets, 1^--2^-_1 , 2^-_2-3^- and 0^+-1^+ state, of ${}^{10}_{\Lambda}$Be. The measurement for ${}^{10}_{\Lambda}$Be was done at JLab and the analysis is in progress. The energy spillitings of these states are predicted to be 0.08 MeV, 0.05 MeV and 0.2 MeV, respectively. Then, it would be difficult to observe the energy splittings for the negative parity which are produced by (K^-, π^-) experiment, although these energy splittings would be helpful for extracting information about the ΛN spin-dependent components.

(2) The effect of the glue-like role of the Λ particle can be demonstrated in ${}^{10}_{\Lambda}$B and ${}^{10}_{\Lambda}$Be. The ground state of ^{9}B is a resonant state. Due to the presence of the Λ particle, the ground state of the resultant hypernucleus ${}^{10}_{\Lambda}$B becomes bound by about 2.0 MeV below the ${}^{9}_{\Lambda}$Be+p threshold. When the Λ particle is added to the bound ground state of ^{9}Be, the corresponding state of ${}^{10}_{\Lambda}$Be becomes bound more deeply by about 4 MeV below the ${}^{9}_{\Lambda}$Be+n threshold. Furthermore, by adding the Λ particle to the resonant state of ^{9}Be, $1/2^+$ and $5/2^-$, the corresponding states of ${}^{10}_{\Lambda}$Be become bound. Especially, we find that the order of the 3^-, 2^-_2, 0^+ and 1^+ states is reversed from ^{9}Be to ${}^{10}_{\Lambda}$Be. From the calculated values of the rms radii $\bar{r}_{\alpha-\alpha}$ and $\bar{r}_{\alpha-\Lambda}$ of ^{9}Be and ${}^{10}_{\Lambda}$Be, we find the shrinkage effect due to the addition of Λ to the core nucleus.

Such an effect was already confirmed by at KEK-E419 experiment.[31] Another interesting feature seen in our result is the three-layer structure of the matter distributions in isodoublet hypernuclear states, being composed of a 2α core, a Λ, and a nucleon. Also, we have neutron halo structures for the 0^+ and 1^+ states.

(3) The charge symmetry breaking effect in ${}^{10}_{\Lambda}$Be and ${}^{10}_{\Lambda}$B are investigated quantitatively on the basis of the phenomenological CSB interaction, which describe the experimental energy difference between $B_\Lambda({}^4_\Lambda\mathrm{H})$ and $B_\Lambda({}^4_\Lambda\mathrm{He})$, Δ_{CSB}. We introduce $\Delta B_\Lambda = B_\Lambda({}^{10}_{\Lambda}\mathrm{Be}) - B_\Lambda({}^{10}_{\Lambda}\mathrm{B})$. And we obtained $\Delta B^{\mathrm{cal}}_\Lambda$ to $-0.02 \sim 0.22$ MeV without and with the CSB interaction, which agree with the observed $\Delta B^{\mathrm{exp}}_\Lambda$ within the large error bar.

In order to elucidate CSB effects in light hypernuclei, it is necessary to have precise data for ${}^{4}_{\Lambda}$H, ${}^{4}_{\Lambda}$He, ${}^{7}_{\Lambda}$He, ${}^{7}_{\Lambda}$Li ($T = 1$), ${}^{7}_{\Lambda}$Be, ${}^{10}_{\Lambda}$Be, and ${}^{10}_{\Lambda}$B. The calculated Λ separation energies of p-shell hypernuclei became inconsistent with the observed data when we use the even-state CSB interaction to reproduce the observed data of s-shell Λ hypernuclei of ${}^{4}_{\Lambda}$H and ${}^{4}_{\Lambda}$He.

In this contradictory situation, one possibility is to re-investigate the experimental data, especially those of ${}^{4}_{\Lambda}$H, ${}^{4}_{\Lambda}$He. At J-PARC, it is planned to measure the M1 transition from the 1^+ state to the 0^+ state in ${}^{4}_{\Lambda}$He at E13 J-PARC project[32] and to measure Λ separation energy of the 0^+ state in ${}^{4}_{\Lambda}$H at Mainz and JLab. From these

measurements, we can investigate the interesting issue of whether or not there is a CSB effect in the binding energies of ${}^{4}_{\Lambda}$He and ${}^{4}_{\Lambda}$H. These experimental results have to affect the CSB effect in p-shell Λ hypernuclei.

As a working assumption to explain the CSB effects both in A=4 and p-shell systems, we have introduced the extremely-repulsive odd-state CSB interaction to cancel out the even-state CSB contributions. Even if this assumption works well, it is an open problem to elucidate physical reality for it. In order to find the effects of the odd-state CSB in $A = 10$ hypernuclei, we need data with 0.1 MeV resolution. In the case of ${}^{10}_{\Lambda}$B, we propose to perform the experiment ^{10}B $(K^-, \pi^-)^{10}_{\Lambda}$B at J-PARC in the future. In the case of ${}^{10}_{\Lambda}$Be, the experiment of ^{10}B $(e, e'K^+)^{10}_{\Lambda}$Be at JLab was done and analysis is in progress. We hope to have the Λ separation energy for this hypernucleus with 0.1 MeV resolution.

Acknowledgments

The authors thank Professors O. Hashimoto, H. Tamura, and S. N. Nakamura, T. Motoba, B. F. Gibson, and D. J. Millener for helpful discussions. This work was supported by a Grants-in-Aid for Scientific Research from Monbukagakusho of Japan(21540288, 20105003). The numerical calculations were performed at the Yukawa Institute Computer Facility HITACHI-SR16000 and KEK-SR16000.

References

1) E. Hiyama, Y. Kino and M. Kamimura, Prog. Part. Nucl. Phys. **51** (2003), 223.
2) E. Hiyama, M. Kamimura, T. Motoba, T. Yamada, and Y. Yamamoto, Phys. Rev. Lett. **85**, 270 (2000).
3) E. Hiyama, Y. Yamamoto, Th. A. Rijken, and T. Motoba, Phys. Rev. C**74**, 054312 (2006).
4) H. Tamura *et al.*, Nucl. Phys. **A754**, 58c (2005).
5) D.J. Millener, Lecture Notes in Physics **724**, 31 (2007); Nucl. Phys. **A804**, 84 (2008);
6) D. J. Millener, Nucl. Phys. **A835**, 11 (2010).
7) R.H. Dalitz and F.Von Hippel, Phys. Lett. **10**, 153 (1964).
8) R.H. Dalitz, R.C. Herndon and Y.C. Tang, Nucl. Phys. **B47**, 109 (1972).
9) S.A. Coon and P.C. McNAMEE, Nucl.Phys. **A322**, 267 (1979).
10) A.R. Bodmer and Q.N. Usmani, Phys. Rev. **C31**, 1400 (1985).
11) A. Nogga, H. Kamada and W. Glöckle, Phys. Rev. Lett. **88**, 172501 (2002).
12) P.M. M. Maessen, Th. A. Rijken, and J. de Swart, Phys. Rev. C **40**, 2226 (1986).
13) Th. A. Rijken, V. G. J. Stoks, and Y. Yamamoto, Phys. Re. C **59**, 21 (1999).
14) A. Gal, Adv. Nucl. Sci. **8**, 1 (1977).
15) B. F. Gibson and E. V. Hungerford III, Phys. Rep. **257**, 349 (1995).
16) O. Hashimoto *et al.*, Journal of Phys. :Conference Series **312** 022015 (2011).
17) JLab E01-011 collaboration, to be submitted in Physical Review Letter.
18) S. Saito, Prog. Theor. Phys. **41**, 705 (1969).
19) M. Kamimura, Phys. Rev. A**38**, 621 (1988).
20) H. Kameyama, M. Kamimura and Y. Fukushima, Phys. Rev. C**40**, 974 (1989).
21) V. I. Kukulin, V. N. Pomerantsev, Kh. D. Razikov, V. T. Voronchev, and G. G. Ryzhinkh, Nucl. Phys. **A586**, 151 (1995).
22) H. Kanada, T. Kaneko, S. Nagata, and M. Nomoto, Prog. Theor. Phys. **61**, 1327 (1979).
23) M. N. Nagels, T. A. Rijken, and J. J. deSwart, Phys. Rev. D **15**, 2547 (1977); **20**, 1633 (1979).
24) E. Hiyama, M. Kamimura, T. Motoba, T. Yamada, and Y. Yamamoto, Prog. Theor. Phys. **97** (1997) 881.
25) E. Hiyama, Y. Yamamoto T. Motoba, and M. Kamimura, Phys. Rev. C**80**, 054321 (2009).
26) A. Hasegawa and S. Nagata, Prog. Theor. Phys. **45**, 1786 (1971).

27) E. Hiyama, M. Kamimura, Y. Yamamoto, and T. Motoba, Phys. Rev. Lett. **104**, 212502 (2010).
28) O. Hashimoto, S.N. Nakamura, L. Tang, J. Reinhold *et al.*, JLab E05-115 proposal, "Spectroscopic investigation of hypernuclei in the wide mass region using the $(e, e'K^+)$ reaction" (2005).
29) T. Motoba, H. Bando, and K. Ikeda, Prog. Theor. Phys. 70, 189 (1983); T. Motoba, H. Bando, K. Ikeda, and T. Yamada, Prog. Theor. Phys. Suppl.81, 42 (1985).
30) E. Hiyama, M. Kamimura, K. Miayazaki, and T. Motoba, Phys. Rev. C**59**, 2351 (1999).
31) K. Tanida *et al.*, Phys. Rev. Lett. **86**, 1982 (2001).
32) H. Tamura *et l.*, J-PARC proposal on 'γ-ray spectroscopy of light hyprnuclei' E13.